Exchange and Inversion in 2-Methylbutyllithium: Proton Nuclear Magnetic Resonance Line Shapes at 300 MHz

Gideon Fraenkel,* William E. Beckenbaugh, and Ping Pin Yang

Contribution from the Department of Chemistry, The Ohio State University, Columbus, Ohio 43210. Received February 13, 1976

Abstract: Molecular weight measurements establish 2-methylbutyllithium (RLi) to be a hexamer in pentane solution. Proton NMR line-shape studies at 300 MHz strongly support a symmetrical octahedral structure. At 300 MHz the racemic reagent evidences two magnetically nonequivalent sets of diastereomeric reagents in ratio 3:2. Under these conditions (*R*)-RLi gives rise to a single species from the NMR spectrum. Two exchange processes at equilibrium bring about changes in the NMR line shape of racemic RLi. They are inversion at carbon bonded to lithium and the exchange of RLi moieties between magnetically inequivalent sites. In contrast (*R*)-RLi shows effects only from inversion. The NMR line shapes have been analyzed using the permutation of indices method to incorporate effects due to different exchange processes. Rate constants extricated from the NMR line shapes for these two processes yield $\Delta H^{\ddagger}$ and $\Delta S^{\ddagger}$ for inversion ca. 15 kcal/mol and ~0 eu and for exchange 3.3 kcal/mol and −34 eu. The significance of these parameters is discussed and it is concluded that the two processes are not correlated.

Alkyllithium compounds[1,2] exist as tetramers or hexamers in hydrocarbon solvents.[3] The symmetrical bridged octahedral structure proposed for primary alkyllithiums on the basis of colligative, infrared, and NMR data[4] has now been revealed with x-ray diffraction methods to describe the crystalline hexamers of cyclohexyllithium and trimethylsilyllithium.[5,6]

Primary alkyllithium compounds at equilibrium in solution undergo fast carbon–lithium bond exchange[1,7] as well as inversion at carbon bonded to lithium.[8,9] The short-lived labile character of the bridged bonds in these aggregates is well documented from ^{1}H and ^{7}Li NMR line-shape studies of mixtures of organolithium compounds.[1,7] For instance, the averaging of the two ^{7}Li resonances in mixtures of methyllithium and ethyllithium allowed measurement of the intermolecular exchange rate of ^{7}Li between the two kinds of aggregates.[10] Also proton NMR line-shape studies of the CH_2Li portion in neohexyllithium and 2-methylbutyllithium[9] provided the rates of inversion at carbon bonded to lithium.

It is of interest to find out whether bond exchange and inversion are correlated processes. Altogether not a great deal is known about the mechanisms of these exchange reactions.

In this paper we show how both inversion and interaggregate exchange can be studied in one and the same compound, thus obviating the experimental interpretive difficulties of dealing with mixtures.

In our earlier studies of inversion in *dl*-2-methylbutyllithium[9] we noticed the low temperature spectra (CH_2Li part) contained unusually broad lines compared to other organometallic compounds of this series.[11] This could arise from several effects, most important of which are scalar ^{7}Li,H coupling and the possible existence of magnetically nonequivalent diastereomeric aggregates. At higher temperatures the line averaging would result from intermolecular exchange of RLi moieties between different magnetic environments superposed on the inversion process at carbon bonded to lithium. Then, in principle, simulation of the NMR line shape for different exchange mechanisms should give the rate constants for the different steps. Such effects should be far more profound at high fields, so we have now tested this hypothesis with NMR line shapes at 300 MHz.

Herein we demonstrate for the first time fine structure in the proton NMR spectrum of a pure organolithium compound as a result of chemical shifts among diastereomeric aggregates. It will be shown how, using our permutation of indices (PI) method,[12] rate constants for inversion and exchange can be extricated from the NMR line shapes.

Results and Discussion

The reaction of 2-methylbutyl bromide with metallic lithium in pentane gave 2-methylbutyllithium (RLi) in over 95% conversion. In this way, starting with *d* (80% optical purity) and *dl* bromide, pentane solutions were obtained of (*R*)-RLi and racemic RLi (**1**). These solutions have been examined with the techniques of NMR spectroscopy, both ^{1}H and ^{7}Li.

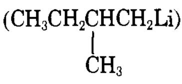

$$(CH_3CH_2\underset{\displaystyle CH_3}{\underset{|}{C}}HCH_2Li)_n$$

1

NMR Data Slow Exchange. Figure 1 displays 60-MHz proton spectra for the CH_2Li portion of (*R*)-RLi and racemic RLi, 1.5 M in pentane, −60 °C. The two spectra are almost identical. In contrast to these results the 300-MHz spectra for the two reagents are entirely different (see Figures 2 and 3). The optically active reagent, (*R*)-RLi, gives rise to a typical AB part of an ABX spectrum (−51 °C, Figure 2) whose parameters are not much different from these obtained for other substituted alkanes. This system is almost first order due to the high magnetic field of the NMR spectrometer. Analysis of the partial spectrum, using computer program LACOON,[13] gives the parameters listed in Table I, and the simulation is shown in Figure 2. It should be mentioned that to reproduce this spectrum from theory it is necessary to use a rather short phenomenalogical T_2. This observation will be discussed in greater detail below.

In contrast to the clean, well-defined appearance of the spectrum of (*R*)-RLi, that of the racemic mixture at −51 °C presents a collection of lumpy, though structured blobs (see Figure 3). The association of alkyllithium compounds to aggregates containing 4–6 RLi units is well documented[3] and there is every reason to believe that 2-methylbutyllithium is subject to the same effects. Then the broadened appearance of the spectrum of *dl*-RLi clearly demonstrates the existence of two or more sets of magnetically nonequivalent diastereomeric aggregates.[14] This spectrum may be best simulated as arising from two overlapping ABX systems in the concentration ratio 3:2 (see Tables II and III). The line-width parameter T_2 needed to match the simulated to the experimental spec-

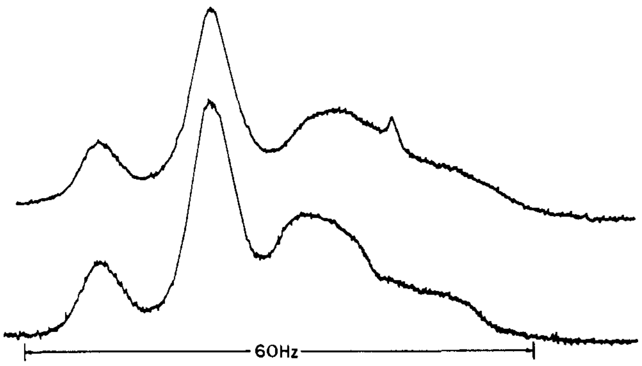

Figure 1. Proton NMR absorption, 60 MHz, −60 °C, CH_2Li portion of 2-methylbutyllithium (RLi), 1.5 M in pentane: top, (*R*)-RLi; bottom, racemic RLi.

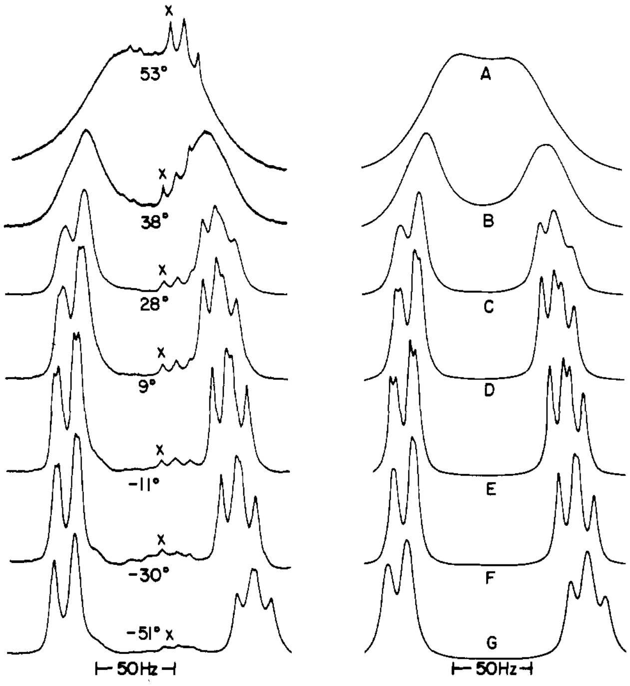

Figure 2. Left, proton NMR absorption, 300 MHz, CH_2Li portion of (*R*)-2-methylbutyllithium, 1.5 M in pentane, at different temperatures, impurities marked with X. Right, NMR line shapes calculated using the parameters listed by temperature in Tables I and VI.

trum (0.085 s) is almost the same as that used for optically active RLi (0.09 s). Figure 3 shows the simulated line shape for *dl*-RLi.

At this point it is useful to speculate on the origin of the broad lines in these NMR spectra of RLi. Their width is certainly not the result of viscosity or field inhomogeneities. That is decisively contradicted by the narrow lines observed for protons other than CH_2Li in the reagent as well as those in the solvent. Most likely ^{7}Li,^{1}H coupling is the cause responsible for line broadening and in fact such effects have been observed before.[2,7]

The possibility of scalar ^{7}Li,H coupling in RLi has been investigated using ^{7}Li NMR. The lithium resonances all consist of single lines whose width increases as the temperature is lowered: for a 1.5 M solution of (*R*)-RLi, 6.7 Hz (23 °C), 13.1 Hz (−36 °C), and 28 Hz (−64 °C); for racemic RLi, 10.4 Hz (23 °C), 13.5 Hz (−36 °C), and 27 Hz (−64 °C). While these results argue in favor of ^{7}Li quadrupole relaxation effects superposed on ^{7}Li,^{1}H scalar coupling, they do not prove it unequivocally.

Finally it could be argued that small shifts due to magnetically nonequivalent sites within the aggregate could bring about these broad lines. But such an effect would be unlikely to bring about the symmetrical (Lorenzian) lines we utilize to simulate the low-temperature spectrum of (*R*)-RLi. Furthermore, racemic RLi, consisting of several diastereomeric aggregates, would then require even broader lines than (*R*)-RLi alone. Since the spectra for both reagents require the same line widths, it would appear that experimentally *we cannot*

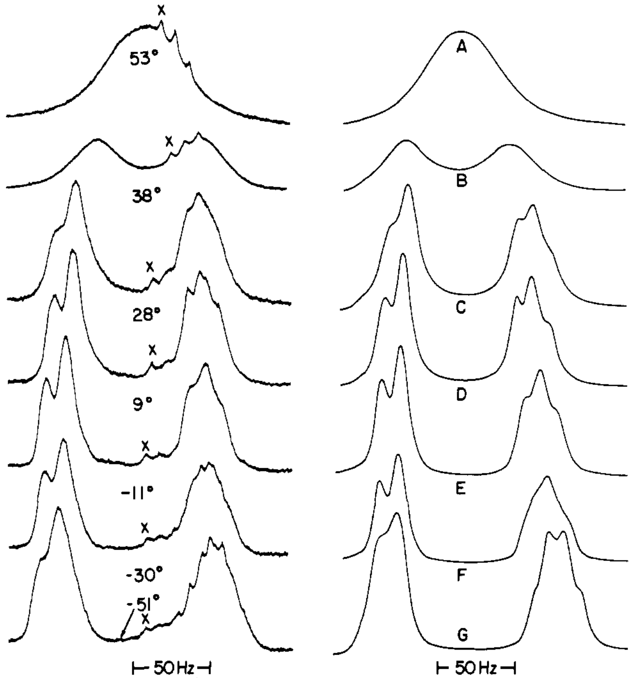

Figure 3. Left, proton NMR absorption, 300 MHz, CH_2Li portion of racemic 2-methylbutyllithium, 1.5 M in pentane, at different temperatures, impurities marked with X. Right, NMR line shapes calculated using the parameters listed by temperature in Tables II, III, and VII.

Table I. NMR Parameters[a] (300 MHz) for (*R*)-2-Methylbutyllithium (1.5 M)

T, °C	ν(X)	ν(A)	ν(B)	$J_{A,B}$	$J_{A,X}$	$J_{B,X}$
53	−150	70.0	153.5	12.9	3.0	9.8
38	−150	70.0	159.5	12.9	3.0	9.8
28	−150	70.0	163.5	12.9	3.0	9.8
9	−150	70.0	165.3	12.9	3.0	9.8
−11	−150	70.0	174.0	12.9	3.0	9.8
−30	−150	70.0	180.0	12.9	3.0	9.8
−51	−150	70.0	191.5	12.7	3.0	9.8
−60	−150	70.0	198.0	12.7	3.0	9.8

[a] Values are given in hertz.

Table II. Chemical Shifts[a] (300 MHz) for *dl*-2-Methylbutyllithium (1.5 M)

T, °C	ν($X_{1,2}$)	ν(A_1)	ν(A_2)	ν(B_1)	ν(B_2)
		Averaged Values			
53	−150	70.0		146.5	
38	−150	72.6		156.9	
28	−150	70.0		157.3	
		Resolved Values			
9	−150	63.0	55.0	153.2	147.2
−11	−150	63.0	55.0	159.2	149.2
−30	−150	63.0	55.0	164.5	154.5
−51	−150	63.0	55.0	172.5	162.5

[a] Chemical shifts are given in hertz.

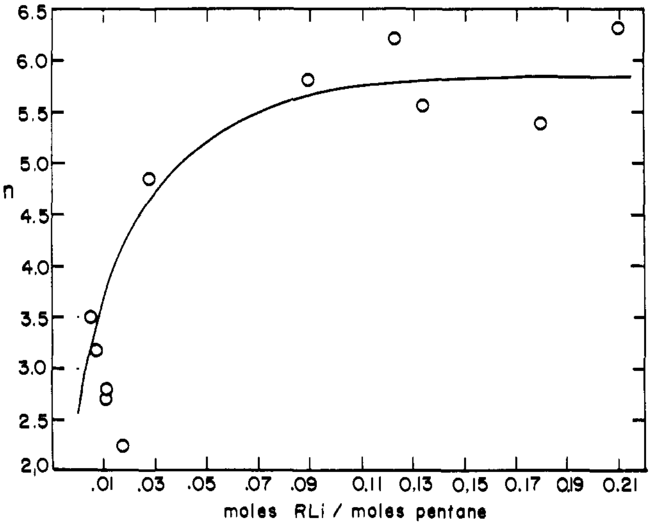

Figure 4. Association number of racemic 2-methylbutyllithium in pentane at 18 °C vs. concentration.

Table III. Coupling Constants[a] (300-MHz Data) for *dl*-2-Methylbutyllithium (1.5 M)

T, °C	J_{A_1,B_1}	J_{A_2,B_2}	J_{A_1,X_1}	J_{A_2,X_2}	J_{B_1,X_1}	J_{B_2,X_2}
			Averaged Values			
53	12.9		3.0		9.8	
38	12.9		3.0		9.8	
28	12.9		3.0		9.8	
			Resolved Values			
9	13.0	13.0	3.3	3.3	9.7	9.7
−11	13.0	13.0	3.3	3.3	9.8	9.8
−30	13.0	13.0	3.4	3.4	9.8	9.8
−51	13.0	13.0	3.3	3.3	9.8	9.8

[a] Chemical shifts are given in hertz.

Table IV. Association Numbers for *dl*-2-Methylbutyllithium in Pentane at Different Temperatures

RLi, M	T, °C	n
0.89	18	6.2
0.89	−5	7.5
0.89	−12	7.6
0.086	18	2.7
0.048	18	3.2

detect magnetically nonequivalent sites within these aggregates. That could, but need not, imply that the aggregates themselves are spherically symmetrical.

Molecular Weight Determinations. In order to gain more insight into the structures of those RLi aggregates it is necessary to know the degree of association. We have accordingly determined molecular weights of 2-methylbutyllithium using the differential pressure technique on the same samples used for NMR. Degassed thermostated vials containing solvent and RLi solution each in contact with one side of an MKS Baratron pressure transducer were equilibrated over several hours (see Experimental Section). These measurements, obtained as a function of concentration, are plotted in Figure 4. The degree of association increases with reagent concentration, in sigmoidal fashion, reaching a maximum of around six by 0.4 M RLi. This is the association number most commonly found for alkyllithiums in hydrocarbon solvents.[3] At lower concentration there appears to be a distribution of smaller species, since the average value of n drops as low as 2.5.

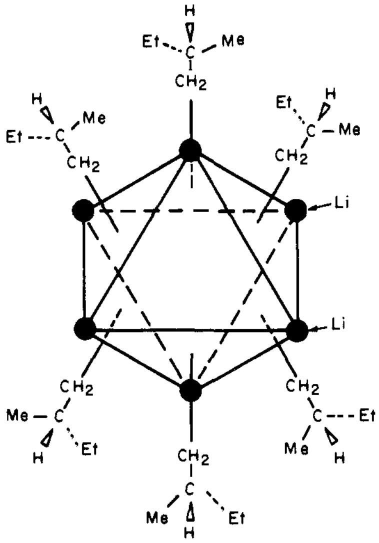

Figure 5. Symmetrical octahedral structure of 2-methylbutyllithium hexamer.

The measurement of differential pressure in our apparatus is easily accomplished at different temperatures and Table IV shows (for the first time) how lowering the temperature increases the association number.

One can probably assume that qualitatively the association behavior of other alkyllithiums in hydrocarbons is similar to that of 2-methylbutyllithium and that the association number increases as the temperature is lowered and decreases on dilution of the sample. One might expect that such variations in the aggregation of organolithium compounds should bring about changes in their chemical reactivity. Such effects must be partially responsible for the fact that even the qualitative chemistry of organolithium compounds depends critically on reaction conditions such as temperature and concentration.[2]

Structure of the Organolithium Aggregate. Altogether we have established that the state of aggregation of 2-methylbutyllithium under the conditions in which the NMR measurements were made is six. Then the simplest interpretation of our NMR data is that the 2-methylbutyllithium hexamer consists of a symmetrical octahedron with CH_2Li moieties occupying the apices and the lithiums positioned in the centers of the triangular planes bounded by three CH_2Li carbons. That is, each lithium is bonded to three carbons (Figure 5). Such a structure with two symmetrically interlocking octahedra has been proposed several times before[4] and confirmed in the cases of cyclohexyllithium[5] and trimethylsilyllithium[6] with x-ray crystallography.

Abbreviated diagrams for part of the set of diastereomeric aggregates of $(RLi)_6$, taking the symmetrical octahedral structure, are displayed in Figure 6. For simplicity the lithiums have been left off and the alkyl groups labeled by absolute configuration R and S. This gives S_6, S_5R, S_4R_2, S_3R_3, S_2R_4, SR_5, and R_6, of which we display the first four since the rest are enantiomers. We assume a random distribution of (R)- and (S)-RLi moieties among the available sites. This results in a binomial distribution of the different aggregates (see Figure 6), the numbers being the coefficients in the expansion of $(x + y)^6$. Table V lists the structurally inequivalent hexamers and their fractional populations.

It is seen that 78% of the material exists as the $R_2S_4 + R_4S_2$ and R_3S_3 species and the ratio of the two is 3:2. This is precisely the ratio of the two magnetically nonequivalent species inferred to comprise the NMR spectrum of *dl*-RLi. Alternatively a 50:50 mixture of $(R_4S_2 + R_2S_4 + R_3S_3)a$ and $(R_4S_2 + R_2S_4 + R_3S_3)b$ would give a less satisfactory fit to the data.

Table V. Inequivalent Hexamers of (RLi)$_6$

Species	Fractional population
$S_6 + R_6$	2/64
$S_5R + SR_5$	12/64
$S_4R_2a + S_2R_1a$	15/64
$S_4R_2b + S_2R_4b$	15/64
S_3R_3a	10/64
S_3R_3b	10/64

To dwell further on which collection of diastereomeric hexamers has a common set of NMR parameters is not worthwhile. It is sufficient to conclude that 2-methylbutyllithium in pentane around 0.9 M associates into hexamers and that a symmetrical octahedral structure is consistent with the low-temperature NMR data.

Effects Due to Exchange Processes. Above −50 °C the NMR spectra of 2-methylbutyllithium undergo familiar changes of line broadening and coalescence associated with the effects due to exchange processes at rates which lie on the NMR time scale. In the case of (*R*)-RLi the process which brings about the averaging of the AB shift and *J*(AB) and the averaging of *J*(AX) with *J*(BX) is undoubtedly inversion at the CH$_2$Li carbon. However, for racemic RLi there are two processes taking place. Within the lower temperature range −30 to 9 °C an exchange process is averaging the NMR parameters for the two magnetically different sets of diastereomeric hexamers. We interpret this to mean that RLi moieties are being transferred reversibly between two environments, each described by its own Hamiltonian.

As a result of new developments in theory and computational simplifications, it is now possible to calculate NMR line shapes for exchanging systems undergoing any kind of intra- or intermolecular exchange process or any combination thereof. The key features to these developments are the use of the product representation and the permutation of indices (PI) to method to include exchange effects.[12]

Herewith we summarize the NMR line-shape calculations for the exchanging 2-methylbutyllithium system studied in this work. First, consider the (*R*)-RLi undergoing inversion only. The organolithium reagent is simulated as a three-spin system, ABX, of which we need only plot the AB part. The eight states of this system are $\alpha_A\alpha_B\alpha_X$ (1), $\alpha\alpha\beta$ (2), $\alpha\beta\alpha$ (3), $\beta\alpha\alpha$ (4), $\beta\beta\alpha$ (5), $\beta\alpha\beta$ (6), $\alpha\beta\beta$ (7), and $\beta\beta\beta$ (8), and the $\Delta m = 1$ transitions between states are:

$$\begin{array}{ccccc} 2 \rightarrow 1 & 5 \rightarrow 2 & 5 \rightarrow 3 & 5 \rightarrow 4 & 8 \rightarrow 5 \\ 3 \rightarrow 1 & 6 \rightarrow 2 & 6 \rightarrow 3 & 6 \rightarrow 4 & 8 \rightarrow 6 \\ 4 \rightarrow 1 & 7 \rightarrow 2 & 7 \rightarrow 3 & 7 \rightarrow 4 & 8 \rightarrow 7 \end{array}$$

To calculate the absorption we need the sum

$$\begin{aligned} \mathrm{Abs}(w) = Im(&\rho_{1,2} + \rho_{1,3} + \rho_{1,4} + \rho_{2,6} + \rho_{2,7} \\ &+ \rho_{3,6} + \rho_{2,7} + \rho_{4,5} + \rho_{5,8} + \rho_{6,8} + \rho_{7,8}) \end{aligned} \quad (1)$$

The density matrix equations in element form are given as

$$\rho_{i,k} = 0 = \mathrm{i}[\rho,\mathcal{H}]_{i,k} - (\rho_{i,k}/T_2) + k_i(\rho_{i,k}(\mathrm{ai}) - \rho_{i,k}) \quad (2)$$

where $m_i - m_k$, 1, k_i refers to inversion, ai refers to after inversion, and $1/T_2$ is the phenomenological line width. The Hamiltonian in the rotating frame is

$$\begin{aligned} \mathcal{H} = \sum_s (\omega - \omega_s)I_s{}^z + J_{\mathrm{A,B}}I_\mathrm{A} \cdot I_\mathrm{B} + J_{\mathrm{A,X}}I_\mathrm{A} \cdot I_\mathrm{X} \\ + J_{\mathrm{B,X}}I_\mathrm{B} \cdot I_\mathrm{X} + \phi_1 \sum_{s=\mathrm{A,B,X}} I_s{}^x \end{aligned} \quad (3)$$

where ϕ_1 is the power of the ratio frequency field in radians per second, ω_s's are shifts, and ω is the observing frequency. The contribution of exchange processes to the line shape enters in the ρ(ai) term. We first note that the product representation is used. Product function ϕ_{ABX} is written $a_\mathrm{A}b_\mathrm{B}x_\mathrm{X}$, the lower case letters being α and β and the order indicates the labeling (capital letters). To evaluate ρ(ai) for the inversion process one permutes the labels of *a* with *b* (which is what happens in the inversion process).

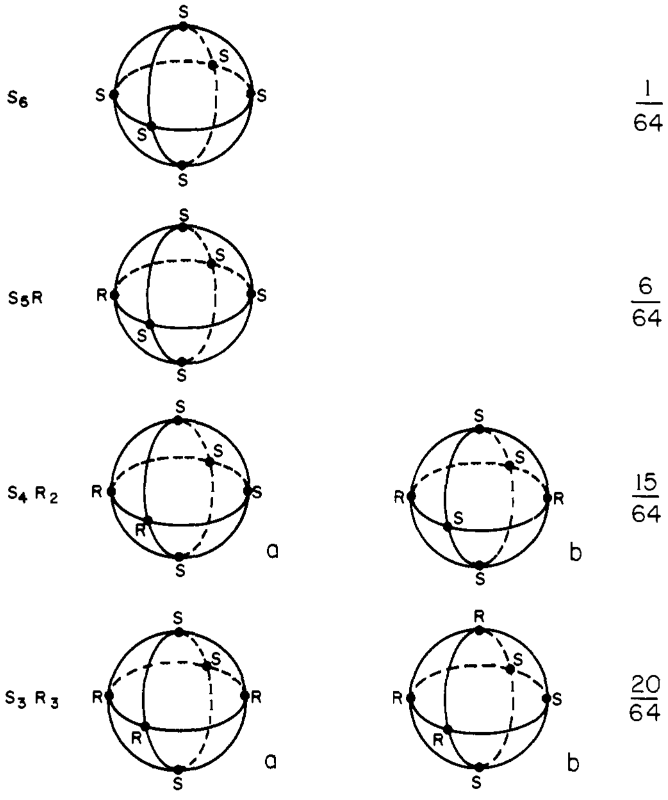

Figure 6. Diastereomeric hexameric aggregates of racemic 2-methylbutyllithium and their distribution.

$$\rho_{abx,a'b'x'}(\mathrm{ai}) = \rho_{bax,b'a'x'} \quad (4)$$

All *i,k* matrix elements of the density matrix equation (eq.3) are taken where

$$m_i - m_k = 1 \quad (5)$$

This generates the set of 15 inhomogeneous coupled equations first order in the $\rho_{i,k}$ elements. These are solved for the ρ elements as a function of the frequency with standard computer procedures. To give a flavor of the problem two of these equations are hereby displayed.

$$\begin{aligned} \rho_{1,3}\left[i\left(\omega - \omega_\mathrm{B} - \frac{J_\mathrm{AB}}{2} - \frac{J_\mathrm{BX}}{2}\right) - \frac{1}{T_{1,3}} - k_\mathrm{i}\right] \\ + i\rho_{1,2}\frac{J_\mathrm{BX}}{2} + \rho_{1,4}\left[k_\mathrm{i} + i\frac{J_\mathrm{AB}}{2}\right] = \frac{i\beta}{8} \end{aligned} \quad (6)$$

$$\begin{aligned} \rho_{2,6}\left[i\left(\omega - \omega_\mathrm{A} - \frac{J_\mathrm{AB}}{2} + \frac{J_\mathrm{AX}}{2}\right) - \frac{1}{T_{2,6}} - k_\mathrm{i}\right] \\ + \rho_{2,5}i\frac{J_\mathrm{BX}}{2} + \rho_{2,7}\left(i\frac{J_\mathrm{AB}}{2} + k_\mathrm{i}\right) = \frac{i\beta}{8} \end{aligned} \quad (7)$$

In these equations the proportionality constant β is

$$\beta = \hbar\phi_1\omega_0/4\pi kT \quad (8)$$

with ω_0 the spectrometer frequency, *k* the Boltzmann factor, *T* the temperature in degrees kelvin and $1/T_{i,k}$ the line width.

In the case of RLi undergoing both inversion and exchange we consider the system to consist of two magnetically different ABX species, $A_1B_1X_1$ and $A_2B_2X_2$. We need to solve as a function of the frequency for 15 density matrix elements for each species, called $\rho_{i,j}{}^1$ and $\rho_{k,l}{}^2$. The absorption comes from the sum of these elements, each weighted by a concentration factor c_1 or c_2.

$$\mathrm{Abs}(\omega) = c_1 Im \sum_{\text{All } i,j} \rho_{i,j}{}^1 + c_2 Im \sum_{\text{All } k,l} \rho_{k,l}{}^2 \qquad (9)$$

where

$$\begin{aligned} m_i - m_j &= 1 \\ m_k - m_l &= 1 \end{aligned} \qquad (10)$$

The Hamiltonians for the two species are written in similar fashion to eq 3, except now every spin symbol has to carry the extra species label 1 or 2.

$$\begin{aligned} \mathcal{H}^1 = &\sum_{s=\mathrm{A}_1,\mathrm{B}_1,\mathrm{X}_1} (\omega - \omega_s) I_s{}^z + J_{\mathrm{A}_1,\mathrm{B}_1} I_{\mathrm{A}_1} \cdot I_{\mathrm{B}_1} \\ &+ J_{\mathrm{A}_1\mathrm{X}_1} I_{\mathrm{A}_1} \cdot I_{\mathrm{X}_1} + J_{\mathrm{B}_1,\mathrm{X}_1} I_{\mathrm{B}_1} \cdot I_{\mathrm{X}_1} + \phi_1 \sum_{s=\mathrm{A}_1,\mathrm{B}_1,\mathrm{X}_1} I_s{}^x \end{aligned} \qquad (11)$$

A similar equation is written for $\mathcal{H}^2$. This time the density matrix equation, operator notation, has the form, e.g., for $\dot{\rho}^1$,

$$\begin{aligned} \dot{\rho}^1 &= 0 \\ &= i[\rho^1, \mathcal{H}^1] - (1/T_2) + k_\mathrm{e}[\rho^1(\mathrm{ae}) - \rho^1] \\ &\qquad + k_\mathrm{i}[\rho^1(\mathrm{ai}) - \rho^1] \end{aligned} \qquad (12)$$

where ae and ai stand for after exchange and after inversion, respectively, and k_e is the exchange rate constant. The $\rho^1(\mathrm{ai})$ term comes out in the same way as eq 4, while $\rho^1(\mathrm{ae})$ is given by

$$\rho_{k,l}{}^1(\mathrm{ae}) = \rho_{k,l}{}^2 \qquad (13)$$

The treatment for $\dot{\rho}^2$ is similar to that for $\dot{\rho}^1$ and need not be described. The result of taking all matrix elements of the $\dot{\rho}^1$ and $\dot{\rho}^2$ equations is to generate the set of 30 coupled first-order equations. These are solved for the density matrix elements to give the absorption. A sample density matrix equation for the *d,l*-RLi undergoing effects from exchange and inversion is now given:

$$\begin{aligned} &\dot{\rho}_{2,7}{}^1 = 0 \\ &\rho_{2,7}{}^1 \left[i \left(\omega - \omega_{\mathrm{B}_1} - \frac{J_{\mathrm{A}_1,\mathrm{B}_1}}{2} + \frac{J_{\mathrm{B}_1,\mathrm{X}_1}}{2} \right) - \frac{1}{T_{2,7}} - k_\mathrm{e} - k_\mathrm{i} \right] \\ &\quad + \rho_{2,5}{}^1 \, i \frac{J_{\mathrm{A}_1,\mathrm{X}_1}}{2} + \rho_{2,6}{}^1 \left[i \frac{J_{\mathrm{A}_1,\mathrm{B}_1}}{2} + k_\mathrm{i} \right] \\ &\quad - \rho_{3,7}{}^1 \, i \frac{J_{\mathrm{B}_1,\mathrm{X}_1}}{2} - \rho_{4,7}{}^1 \, i \frac{J_{\mathrm{A}_1,\mathrm{X}_1}}{2} + \rho_{2,7}{}^2 k_\mathrm{e} = \frac{i\beta}{8} \end{aligned} \qquad (14)$$

The equation for $\dot{\rho}_{2,7}{}^2$ is generated by replacing in eq 14 the species label 1 wherever it occurs by 2 and 2 by 1.

A computer program has been written to assemble the coefficient matrix of the density matrix equations (**A**)

$$(\omega I + \mathbf{A})\rho_{\mathrm{col}} = i\beta B_{\mathrm{col}} \qquad (15)$$

and plot the line shapes.

The input parameters for these line-shape calculations consist of all shifts, coupling constants, line widths, and rate constants. The simpler system (*R*)-RLi was handled first, since it contains only one magnetically recognizable species. First guesses for the NMR parameters come from the low-temperature spectra. It became evident that the shifts and intrinsic line widths varied in a monotonic manner with the temperature. If the shifts of A and X are assigned to be constant, then B varies with the temperature. At first the NMR parameters were estimated by extrapolating from the low-temperature data. Then finally all parameters were iterated to give the best simulation of the experimental spectra. The NMR parameters from these calculations are listed in Table I, the rate constants and T_2's in Table VI, and the calculated line shapes are shown in Figure 2.

Table VI. Inversion Rate Constants (k_i) and Line-Width Parameters (T_2) for (*R*)-2-Methylbutyllithium, 1.5 M

T, °C	T_2(A), s	T_2(B), s	k_i, s^{-1}
53	0.085	0.085	201
38	0.085	0.085	64
28	0.070	0.070	22
9	0.070	0.070	4
−11	0.070	0.065	0.4
−30	0.065	0.060	0.05
−51	0.057	0.040	*a*
−60	0.050	0.030	*a*

[a] Slow limit.

Table VII. Rate Constants for Inversion and Exchange and Line-Width Parameters for *dl*-2-Methylbutyllithium (1.5 M)

T, °C	T_2, s	k_e, s^{-1}	k_i, s^{-1}
53	0.09		101
38	0.08		38
28	0.07		13
9	0.07	71	6.4
−11	0.07	30	0.2
−30	0.07	20	0.02
−51	0.05	10	*a*
−60	0.05	4	*a*

[a] Slow limit.

Table VIII. Activation Parameters for Exchange and Inversion of 2-Methylbutyllithium (RLi, 1.5 M)

Species process	$\Delta H^{\ddagger}$, kcal/mol	$\Delta G^{\ddagger}$, 281 K	$\Delta S^{\ddagger}$, eu	k, s^{-1} (281 K)
(*R*)-RLi inversion	15.6 ± 1.1	15.8 ± 1	−0.6 ± 3	4.0
(*RS*)-RLi inversion	14.8 ± 1	15.7 ± 1	−3 ± 3	6.4
(*RS*)-RLi exchange	3.3 ± 0.5	13.3 ± 1.5	−39 ± 7	72

The rate constants for inversion in (*R*)-RLi we used among the primary input for calculating the line shapes for racemic RLi, where both inversion and exchange exert effects on the spectra. The analysis was carried out as described above and the final iterated parameters are listed in Table II (shifts) and III (coupling constants). Table VII contains the rate constants and T_2 values. These parameters produce the line shapes shown in Figure 3. Finally, Eyring plots for inversion and exchange are shown in Figures 7 and 8 and the parameters summarized in Table VIII.

The critical feature of these results is the set of shifts among the A and B hydrogens in the two reagents. The AB line shape does not depend on the exact shift of X. Table II shows how for racemic RLi, when X_1 and X_2 are fixed, then the A shifts are constant, while those of B_1 and B_2 increase with the temperature with the same slope. In this way the internal shifts $\delta(A_1) - \delta(A_2)$ as well as $\delta(B_1) - \delta(B_2)$ remain constant.

These results show that 2-methylbutyllithium undergoes two different kinds of processes which bring about averaging of selected NMR parameters—a fast process whereby RLi moieties transfer between two different magnetic environments, which we call interaggregate exchange, and the slower

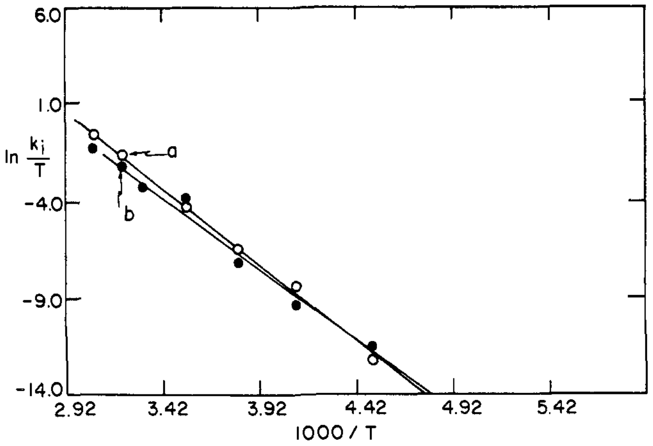

Figure 7. Eyring plots for inversion in *R*, ○, and racemic 2-methylbutyllithium, ●.

process of inversion at carbon bonded to lithium. Although the quantities of activation for the two processes are enormously different, there is a balance of entropy with enthalpy, which results in a $\Delta G^{\ddagger}$ different by ca. 2 kcal/mol. While the two exchange processes can best be studied over different temperature ranges, they both effect the NMR line shape for *dl*-RLi between −11 and 9 °C.

Rate constants for inversion in (*R*)-RLi compared to the racemic reagent are quite similar. One would expect diastereomers to invert at different rates, but in this work the rates are only slightly different. This applies to the activation parameters as well (see Figure 7, Table VII). The almost neutral entropy change accords with our previous finding from 60- and 100-MHz proton spectra that the inversion process is first order in contained RLi.

The activation parameters for the exchange process are subject to larger errors than those for inversion. Even so there is no doubt that the enthalpy of activation is very low and the entropy large and negative.

There are several ways by which two diastereomeric shifts could be averaged. One possibility is a dissociation–recombination mechanism involving hexamers in equilibrium with trimers.

$$R_3S_3 \rightleftarrows R_2S + RS_2 \qquad (16)$$

$$2R_2S \rightleftarrows R_4S_2 \qquad (17)$$

However, the large negative entropy argues against this proposal. The entropy of activation is more consistent with a bimolecular exchange between two hexamers in which two RLi units mutually exchange places.

$$R_3{}^*S_3{}^* + R_2S_4 \rightleftarrows R_2{}^*S_3{}^*S + R^*R_2S_3 \qquad (18)$$

Alternatively one or more rearrangements could take place inside a stable intermediate organolithium dodecamer.

$$R_3{}^*S_3{}^* + R_2S_4 \rightleftarrows R_3{}^*R_2S_3{}^*S_4 \rightleftarrows R_2{}^*S_3{}^*S + R^*R_2S_3 \qquad (19)$$

The NMR line shape for such exchanging systems could be simulated (at great expense), but the results would not distinguish among the different mechanisms. Thus, it is not now worthwhile to speculate further on the nature of this exchange mechanism.

Altogether the evidence favors a large transition state with very little bond breaking and a great deal of order or frozen motion compared, respectively, to the ground-state hexamer.

Conclusion

We have shown by means of proton NMR line-shape analysis at 300 MHz that the 2-methylbutyllithium hexamer undergoes two exchange processes—inversion at carbon bonded to lithium, which takes place inside the aggregate, and, somewhat faster, an exchange which transfers RLi moieties from one aggregate to another. This process is accompanied by little bond breaking and much restriction of motion.

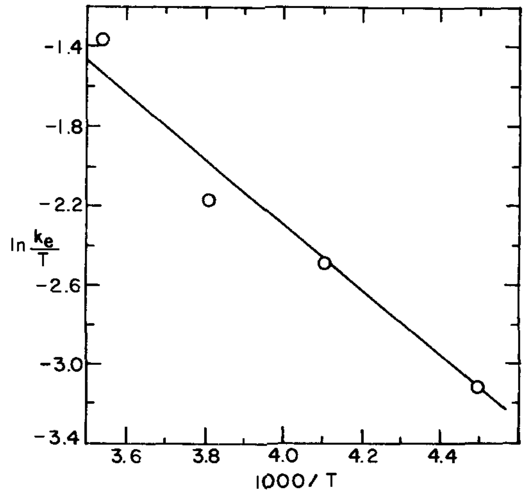

Figure 8. Eyring plot for interaggregate exchange of racemic 2-methylbutyllithium.

The utility of high-field NMR studies of diastereomeric species such as organolithium compounds is highly recommended. It should apply well also to other molecular complexes.

Experimental Section

Chemicals. Pentane was distilled from sodium potassium alloy. Ether was distilled out of a ether solution of butylmagnesium chloride. (*R*)-2-methylbromobutane ($[\alpha]^{20}\Delta$ = 4.65°, 80% optically pure) and the racemic mixture came from K and K Laboratories; these compounds were also prepared from the corresponding alcohols.

Glassware. All glassware, including syringes, was baked out in a 200 °C oven. Glassware used for organometallic preparations was flamed out in a current of argon immediately before use.

***d*-2-Methylbromobutane.** Into a dry 250-ml three-neck flask containing a teflon coated magnet and fitted with a 50-ml addition funnel, condenser, and drying tube (Drierite) were placed *d*-2-methyl-1-butanol (75.1 g, 0.851 mol) and 23.7 ml of reagent-grade pyridine. After cooling to 0 °C with an ice-water slush, phosphorus tribromide (92.7 g, 0.342 mol) was added dropwise over a period of 1 h. The reaction mixture was allowed to warm up to room temperature with stirring. A distilling head was attached and the mixture heated at reduced pressure until no further distillate was collected. This was then mixed with petroleum ether (40–60 °C) and washed in the following sequence with 200 ml of 5% aqueous sodium hydroxide, 200 ml of 10% sulfuric acid, and 200 ml of cold distilled water. The organic layer was dried with magnesium sulfate, the solvent removed with a rotary evaporator, and the residue distilled at 120–121 °C to give 103 g of *d*-2-methyl-1-bromobutane in 80% yield, [α_Δ = 4.6°], 80% optical purity.

(*R*)-2-Methylbutyllithium. A three-neck, 24/40, 250-ml flask containing a teflon-coated magnetic stir bar was equipped with a dry-ice condenser, a side arm bearing a 2-mm straight bore teflon stopcock, an addition funnel (needle valve), and provision for passing through argon. The entire assembly was flamed out in a current of argon. Dry oxygen-free pentane (50 ml) was placed in the reaction vessel. Lithium (4.65 g, 0.67 at wt) wire was cleaned and cut into small pieces under dry pentane and then quickly transferred into the reaction vessel. Pentane was removed with a syringe and the lithium washed in this manner with two further aliquots of pentane. Then 90 ml of pentane was syringed into the reaction vessel. *d*-2-Methylbutyl bromide (33.9 g, 0.225 mol) was purged of air with a current of argon and then syringed into the addition funnel through the protective serum cap, followed by 30 ml of dry oxygen-free pentane. This halide–pentane mixture was slowly released into the reaction vessel over a period

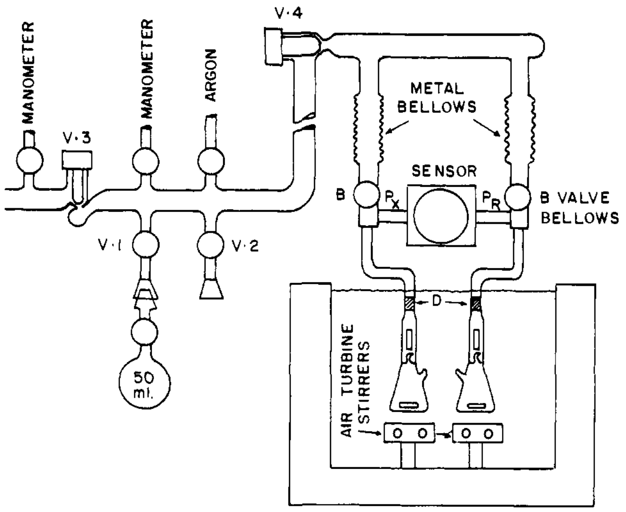

Figure 9. Molecular weight apparatus.

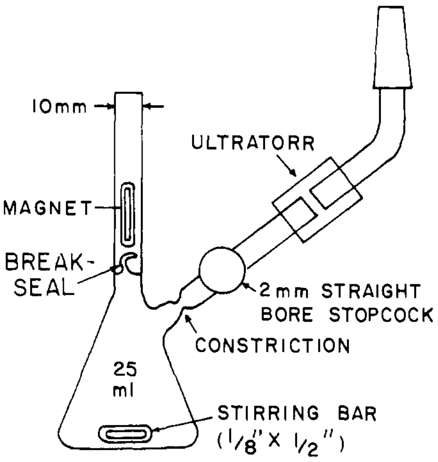

Figure 10. Sample flask used for molecular weight measurements.

of 1 h. After 5 min a cloudy precipitate developed and the lithium turned violet. When addition was over the lithium had turned black and the temperature of the reaction mixture had risen to 30 °C. The system was allowed to stir overnight at room temperature under argon. This procedure gave 150 ml of a solution 1.51 M in 2-methylbutyllithium, less than 0.01 M in alkoxide (Gilman titration), and free of halide (<0.001 M). This solution was used, after suitable dilution, for all the NMR and molecular weight studies. One sample, distilled across a Y-shaped tube on the vacuum line, behaved in the same way as the original solution. Samples for NMR spectroscopy were sealed off under vacuum in 5-mm o.d. precision tubes.

NMR Spectroscopy. Proton NMR spectra were obtained with the Varian HA-100 spectrometer operating in the frequency sweep mode. The 300-MHz spectra were obtained using the Varian HR-300 instrument, internally locked and frequency swept at the Department of Chemistry, University of Akron, Akron, Ohio. This part of the work was carried out with the assistance of Mr. Everett Santee. Lithium NMR data were obtained using the modified HA-100 spectrometer, field sweep mode, at the Department of Chemistry, University of Illinois, Urbana, Ill. with the cooperation of Dr. Paul Loeffler.

Molecular Weight Measurements. The MKS Baratron measures differential pressure mechanically via a stretched steel membrane placed between gas at two different pressures. This is converted to a capacitance value, which can be monitored as a voltage. The measuring unit is read out on a calibrated meter with three range switches and an offset control which can offset up to 100% of the head value. The meter is then used as a null detector, which is zeroed when the offset control matches the value of the differential as measured in percent of the 30.000-mm range of the head.

The complete apparatus shown in Figure 9 includes the MKS measuring head, the attached flasks, valves, vacuum line, and water bath. Figure 10 shows the break seal sample flask used in these studies. This is opened to the head with a iron-in-glass hammer manipulated by an external magnet.

The sample is best prepared by the following procedure. The empty flask is attached to the vacuum line via an Ultratorr connector and glass joint adaptor and flamed out with pumping with the diffusion pump down to 1 × 10^{-5} Torr. Then the flask is removed from the vacuum line, filled with dry argon, weighed, and the sample solution syringed in. At this point, the flask is attached to the vacuum line again and the solvent removed by trap-to-trap distillation and the weight of the organometallic determined. Fresh dry solvent is then syringed into the flask or distilled in. If the material is harmed in some way by evaporation to dryness, then the solution syringed in can simply be degassed and weighed and the weight of compound determined by titration at the end of the experiment. This may also be obtained from the difference between the weight of solution and the weight of all aliquots of solvent distilled off during measurements. The sample is degassed by a minimum of six freeze-pump-thaw cycles.[15] Degassing is complete when opening the stopcock to the frozen flask results in no discernible pressure rise on the vacuum gauge. Then the flask is sealed shut with a flame at point B and carefully annealed. *Care* should be taken to make sure the constriction was previously rinsed with the solvent so that no decomposition occurs during sealing. The glass hammer is carefully slid onto the break seal and the flask attached with a flame to the Kovar-to-glass seal (point D, Figure 10) and annealed. The sample is attached to the P_R side and the pure solvent to the P_X side, so that the differential will be read as a positive number. After opening the bellows valves to the diffusion pump both sides are evacuated, and the glass tubing flamed out. This is necessary to degas the metal tubing and remove water vapor admitted during attachment of the samples. After 0.5 h at the best possible vacuum, the valves are closed tightly by hand, the meter is zeroed with the range switch on the 0.01 setting, and the offset knobs are all set to zero. The procedure in the manual should be followed at this point. The head should be warmed up for at least 12 h prior to beginning measurement to maintain a stable zero point. No needle deflection from zero should be seen. The needle will indicate which side has the greater pressure and this can be checked by opening the side under suspicion to vacuum. The needle should return to zero; retightening the valves usually solves the problem. When one is satisfied the system is tight the flasks are frozen down and the break seals opened followed by reequilibration.

The system is now ready to be equilibrated in a constant-temperature bath. The bath is positioned beneath the flasks and raised via the lab jacks until the flasks come within ⅛ in. or so of the top of the air driven stirrers. The flasks are stirred at 60–100 rpm while the bath is equilibrated. The bath temperature should be at least a few degrees below room temperature to avoid solvent distillation to the upper portions of the apparatus. After about 1 h readings of %(ΔP) can be taken. Readings should be made every 15 min for a period of several hours. This will give a good ΔP_{AVG} for each concentration.

For lower temperatures, the bath is filled with ethylene glycol and cooled directly with the "Adapt-A-Cool" cooling coil. Temperatures of ∼−10 °C can be reached in this manner or using a smaller bath a correspondingly lower temperature.

To change the solute concentration, solvent is distilled from the sample into a previously weighed ampule. Valve 3 is closed and the bellows valve opened very slightly. This valve is then closed and the remaining vapor in the system condensed into the ampule. The pressure of the remaining solvent vapor is monitored with the mercury manometer. The bulb is removed and reweighed at room temperature. Both sample flasks should be refrozen and requilibrated as each aliquot is removed.

The aggregation, n, is given by

$$n = \frac{m_1 w_2}{m_2 w_1} \cdot \left(\frac{1 - \Delta P/P}{\Delta P/P}\right)$$

where m_1 and m_2 are weights of compound and solvent, respectively, w_1 and w_2 their molecular weights, P the vapor pressure of pure solvent, and ΔP the differential pressure measured above. A statistical treatment of the resultant n values has been thoroughly discussed.[15]

The procedure described above gave satisfactory molecular weights for benzophenone with a precision of 1% and reproducible to 0.5%.

NMR Line-Shape Calculations. Calculations of NMR line shape for the 2-methylbutyllithium exchanging and inverting system were carried out at the Ohio State University Computer Center using the IBM 370-105 computer and displayed on a Calcomp plotter. The results in Tables I–VI represent the best fits of calculated to experimental spectra obtained by iterating the NMR parameters and rate constants. The error in the fit was 5% of the rate constant in the coalescence region, where line shape is most sensitive to changes in rate constant, to 10–12% approaching the slow and fast exchange limits.

Acknowledgment. This research was supported by a Grant from the National Science Foundation. We thank Dr. Paul Loeffler and Professor T. L. Brown for their help with the lithium NMR work at the University of Illinois and Mr. Everett Santee, who operated the 300 MHz NMR spectrometer at the University of Akron. This instrument was financed with a special grant from the state of Ohio and maintained partly with funds from the National Science Foundation.

References and Notes

(1) T. L. Brown, *J. Pure Appl. Chem.*, **23**, 447 (1970).

(2) B. J. Wakefield, "The Chemistry of Organolithium Compounds", Pergamon Press, Oxford, England, 1974.

(3) D. Margerison and T. P. Newpont, *Trans. Faraday Soc.*, **59**, 2058 (1963); M. Weiner, C. Vogel, and R. West, *Inorg. Chem.*, 1, 654 (1962); M. L. Lewis and T. L. Brown, *J. Am. Chem. Soc.*, **92**, 4664 (1970).

(4) T. L. Brown, *Adv. Organomet. Chem.*, **3**, 365 (1965).

(5) R. Zerger, W. Rhine, and G. Stucky, *J. Am. Chem. Soc.*, **96**, 6048 (1974).

(6) T. F. Schaaf, W. Butler, M. D. Glick, and J. P. Oliver, *J. Am. Chem. Soc.*, **96**, 7593 (1974).

(7) K. C. Williams and T. L. Brown, *J. Am. Chem. Soc.*, **88**, 4134 (1966); L. M. Seitz and T. L. Brown, *ibid.*, **88**, 4140 (1966); D. P. Novak and T. L. Brown, *ibid.*, **94**, 3793 (1972); R. L. Kieff and T. L. Brown, *J. Organomet. Chem.*, **77**, 289 (1974); R. L. Kieft, D. P. Novak, and T. L. Brown, *ibid.*, **77**, 299 (1974).

(8) M. Witanowski and J. D. Roberts, *J. Am. Chem. Soc.*, **88**, 736 (1966).

(9) G. Fraenkel, D. T. Dix, and M. J. Carlson, *Tetrahedron Lett.*, 579 (1968).

(10) L. M. Seitz and T. L. Brown, *J. Am. Chem. Soc.*, **88**, 2174 (1966).

(11) G. Fraenkel, C. E. Cottrell, and D. T. Dix, *J. Am. Chem. Soc.*, **93**, 1704 (1971).

(12) J. I. Kaplan and G. Fraenkel, *J. Am. Chem. Soc.*, **94**, 2709 (1972).

(13) A. A. Bothner-By, Quantum Mechanics Program Exchange, Department of Chemistry, Indiana University, Bloomington, Ind. Modified for use in the Nicholet 1080 Computer by Dr. J. W. Cooper, Tufts University.

(14) Note that not all diastereomers need be magnetically nonequivalent.

(15) D. Margierson and J. D. Pont, *Trans. Faraday Soc.*, **67**, 353 (1971).

---

^{15}N Nuclear Magnetic Resonance Spectroscopy. The Nebramycin Aminoglycosides

Douglas E. Dorman,* Jonathan W. Paschal, and Kurt E. Merkel

Contribution from the Lilly Research Laboratories and Biochemical Development Division, Eli Lilly and Company, Indianapolis, Indiana 46206.

Received February 17, 1976

Abstract: The ^{15}N NMR spectra of some of the components of the nebramycin complex are reported. Resonances are assigned through comparisons of spectra of the individual factors. The observed chemical shifts are broadly consistent with the current knowledge of substituent effects in ^{15}N NMR spectroscopy. Titration curves can be used to obtain pK_a values for each of the nitrogens of a compound. The results of this study were used to confirm the identification of a monoacetyl derivative of tobramycin.

Recent studies of ^{13}C nuclear magnetic resonance (NMR) of the aminoglycoside antibiotics have vastly simplified the problem of structure elucidations of these compounds.[1] Furthermore, the effect of protonation of the basic amines on ^{13}C chemical shifts[1f] has been used to guide attempts to modify chemically the structure of an aminoglycoside.[2] The recent report of the measurement of ^{15}N NMR spectra of amino sugars[3] indicates yet another potentially useful method of studying the structures and reactivities of the aminoglycoside antibiotics. In this paper, we report our own initial explorations of the ^{15}N NMR spectra of these compounds.

The subjects of the present investigation were some of the various biologically active factors of the nebramycin complex of aminoglycoside antibiotics isolated from *Streptomyces tenebrarius*. The structures of the compounds studied are detailed in Table I. Most of these structures have been established by previous workers;[1f,4] the structures of factors 3 and 7 were established in these laboratories and will be reported elsewhere.[1g]

Experimental Section

^{15}N NMR spectra were measured on a JEOL PFT-100 spectrometer operating at 10.09 MHz and equipped with a ^1H decoupler, a deuterium field-frequency lock, and a JEOL EC-100 data system. The free induction decay was collected into 8K of computer memory, using a spectral width of 5 kHz. Samples were pulsed with a repetition rate of 2 s, using a 45° pulse angle. The conditions of data collection and transformation would be anticipated to contribute ca. 1.7 Hz to the natural line width.

Samples of concentration 0.5–1.0 M were prepared in $H_2O \cdot D_2O$ (ca. 9:1). No special precautions were taken to exclude paramagnetic impurities, and the solutions were not degassed. pH was adjusted, using approximately 6.6 N KOH and HCl solutions.

In some cases, spectra taken in acidic solutions required much longer scanning. At pH 11, a spectrum of apramycin was taken utilizing a decoupling technique designed to retain nuclear Overhauser enhancement without collapsing scalar coupling;[5] this spectrum did not differ in any material way from that obtained from normal noise-modulated proton decoupling.

^{15}N chemical shifts were measured relative to external $^{15}NH_4Cl$ (2.9 M) in 1 M HCl contained in a coaxial 2-mm capillary. In all cases, the resonances of the sample had the same phase as the standard sample.

Results

^{15}N chemical shifts measured in this study are presented in Table II. In acidic or basic solutions, the various nitrogen resonances are well resolved; at some intermediate pH values, peak overlaps occur, but they could easily be detected through their relative peak heights. In the case of apramycin in alkaline solution, the spectrum was remeasured in the absence of the external standard to detect the underlying resonance. Chemical shifts in alkaline solution are probably accurate to ±0.1 ppm. In acidic media, greater peak width reduces the accuracy to 0.2 ppm. In some cases, the pH drifted significantly during